Angular Distribution of Inelastically Scattered Deuterons

JAMES W. HAFFNER*
Laboratory for Nuclear Science, Massachusetts Institute of Technology, Cambridge, Massachusetts
(Received November 21, 1955; revised version received February 20, 1956)

A particle selection technique developed in the MIT cyclotron laboratory has been applied to the study of the angular distributions of inelastically scattered deuterons at a bombarding energy of 15 Mev, the angular distributions of the (d,d') reactions from Li^6 ($Q=-2.19$ Mev), Li^7 ($Q=-4.61$ Mev), Be^9 ($Q=-2.43$ Mev), C^{12} ($Q=-4.43$ Mev), Mg^{24} ($Q=-1.37$ Mev), and Al^{27} ($Q=-2.23$ Mev, $Q=-2.75$ Mev) were obtained. These data were analyzed according to the nuclear interaction theory of Huby and Newns, the electric interaction theory of Mullin and Guth, and from the standpoint of compound nucleus formation. The behavior of the angular distributions indicates that for small angles (large impact parameters) electric interaction contributes appreciably. However, for large angles (small impact parameters) the nuclear interaction theory fits the data better. Consideration of the cross sections involved favors the nuclear interaction theory. Compound nucleus formation does not appear to play a major role in inelastic deuteron scattering. Improved theoretical treatments of the problem should make possible the determination of the spins and parities of nuclear states not easily reached by other reactions.

INTRODUCTION

DEUTERON–INDUCED reactions have been investigated, both theoretically and experimentally, in many ways. However, very few experiments have been done with inelastically scattered deuterons, mainly because elastic deuterons, as well as protons from (d,p) reactions, make the identification of inelastically scattered deuterons a major problem.

The development of a particle selection technique by Aschenbrenner[1] has provided a tool by means of which this problem can be overcome. By separating the deuterons from the protons, the inelastically scattered deuterons can then be identified by their energy.

There have appeared three main theoretical approaches to the inelastic deuteron process. One of these is a modification of the Oppenheimer-Phillips, or stripping, process which assumes that only one member of the deuteron (more probably the neutron) interacts with the target nucleus. During the interaction, however, the deuteron may retain its identity as a particle and be scattered with a diminished energy, the remainder being transferred to the nucleus. The second theory assumes that the energy is transferred from the deuteron to the nucleus by an electric interaction similar to the process of nuclear excitation by electromagnetic radiation. The third approach is by the process of compound nucleus formation.

The object of this investigation has been to obtain information concerning the process of the inelastic scattering of deuterons by obtaining angular distribution and cross sections in (d,d') reactions. Comparison of the data with the predictions of the theories was then used to check the validity of the theories as well as to indicate the relation between (d,d') and other deuteron-induced reactions.

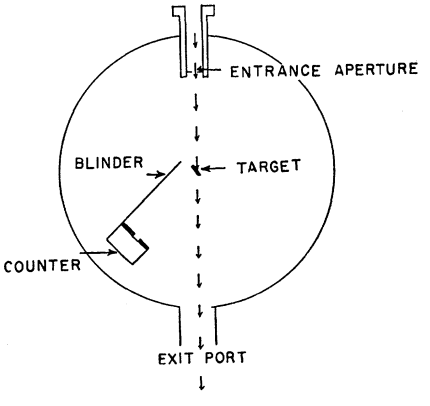

FIG. 1. Schematic diagram of scattering geometry, showing scattering chamber, particle selective counter, and scattering chamber. Deuterons scattered from the entrance slits or the blinder lose sufficient energy that they can be readily distinguished from deuterons scattered inelastically in the target.

EXPERIMENTAL PROCEDURE

A. Cyclotron and Emergent Beam Apparatus

The source of the incident deuterons used for these experiments was the 15-Mev external beam of the MIT cyclotron.[2] The deuterons are conducted through a tube to a scattering chamber. Set inside the tube are a series of tantalum baffles and a defining aperture at the entrance of the scattering chamber. A focusing magnet serves to focus the deuterons on the target at the center of the scattering chamber. This system of baffles and magnet produces a beam-spot on the target approximately $\frac{1}{4}$ inch wide and $\frac{3}{8}$ inch high.

The scattering chamber was a modification of the one used previously.[3] The major differences are: (a) There are 6 large Plexiglas windows around the sides of the chamber. (b) The target capacity has been increased to 4, and the targets can be positioned more

* Now at the General Electric Company, Cincinnati, Ohio.
[1] F. A. Aschenbrenner, Phys. Rev. 98, 657 (1955).
[2] M. S. Livingston, J. Appl. Phys. 15, 2 (1944).
[3] Boyer, Gove, Harvey, Deutsch, and Livingston, Rev. Sci. Instr. 22, 310 (1951).

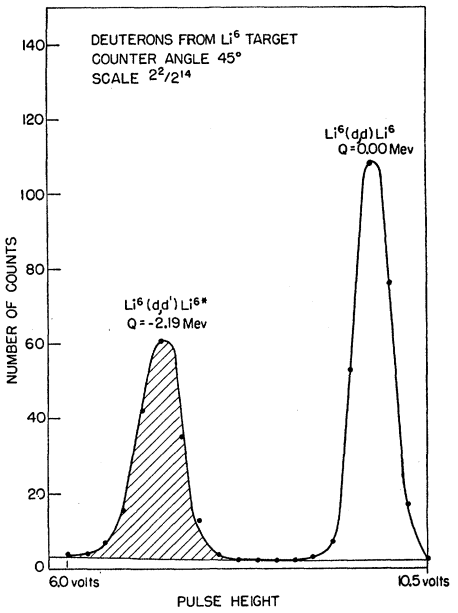

FIG. 2. Scattered deuteron energy spectrum from deuteron bombardment of Li^6 target.

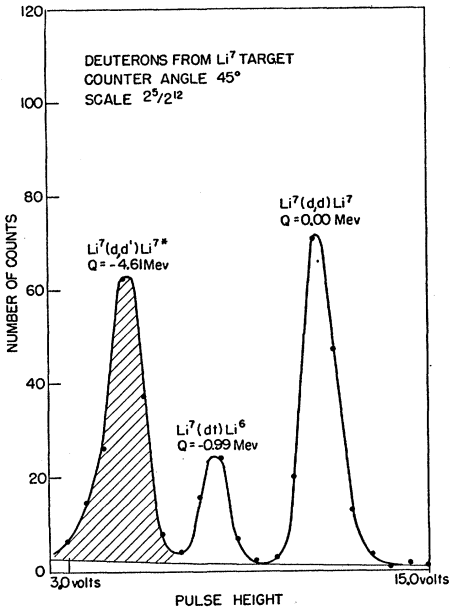

FIG. 3. Scattered deuteron energy spectrum from deuteron bombardment of Li^7 target.

accurately. (c) The angular sensitivity of the counters and of the target have been increased. (d) An evaporating system has been incorporated with the chamber, allowing target material to be evaporated onto a target and bombarded without exposure to air. A schematic diagram of the scattering chamber with the particle selection counter inside is seen in Fig. 1.

B. Particle Selection Technique

The method of particle selection used is a modification of that employed by Aschenbrenner[1] in investigating low-energy protons from (d,p) reactions. Essentially, the system consists of two scintillation counters in series. The first is thin energy-wise so that its output is proportioned to dE/dx, the specific ionization, of the particle. The second is sufficiently thick to stop the particle. Its output is proportional to the total remaining energy of the particle.

Since dE/dx is approximately proportional to z^2/v^2 [4] and $E=\frac{1}{2}Mv^2$, the product of the output of the first counter and the sum of the output of the two counters is proportional to z^2M. This product is obtained by means of a pulse multiplier consisting of a 5×5 matrix of 6BN6 tubes. The product spectrum so obtained was sent through a pulse-height analyzer into one side of a coincidence circuit. The output from the second scintillation counter was fed into the other side of the coincidence circuit.

It was thus possible to obtain energy spectra of any desired charged particle resulting from the deuteron bombardment of the targets (see Figs. 2 to 7). In each case, the peaks studied are believed to correspond to one nuclear energy level. This is because the shape and the location of the peak did not change anomalously. If more than one nuclear energy level is responsible for any of the peaks observed, either one of them predominates over the others for the energy and angles studied, or that they all have the same J value. In Fig. 8 are shown cathode-ray oscilloscope pictures of the energy and mass particle groups. Mass is plotted

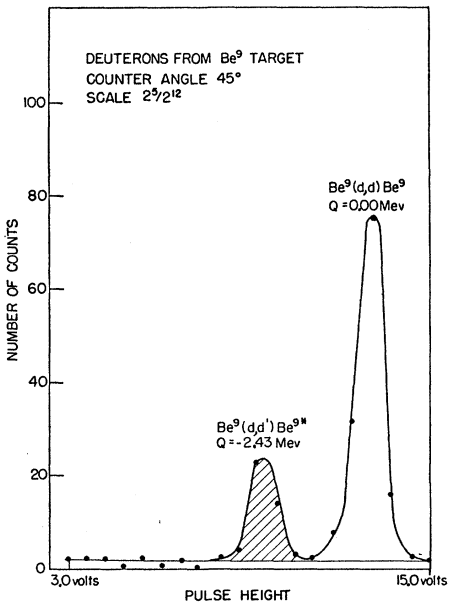

FIG. 4. Scattered deuteron energy spectrum from deuteron bombardment of Be^9 target.

[4] Aron, Hoffman, and Williams, Atomic Energy Commission Report AECU-663 (unpublished).

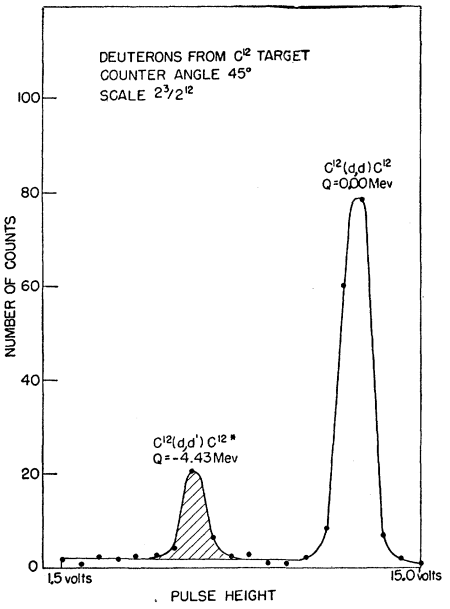

FIG. 5. Scattered deuteron energy spectrum from deuteron bombardment of C^{12} target.

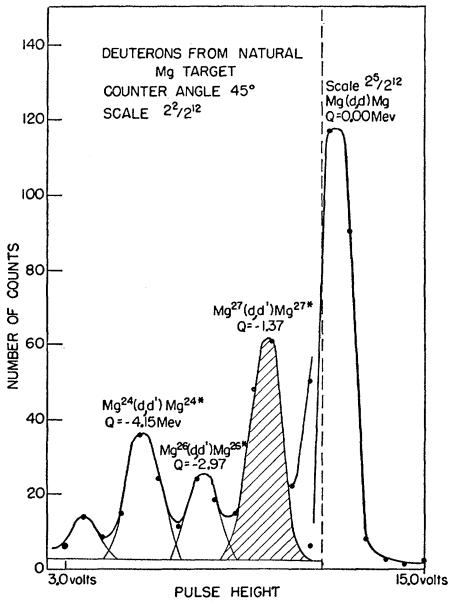

FIG. 6. Scattered deuteron energy spectrum from deuteron bombardment of natural Mg target.

horizontally, energy vertically. By inverting the photograph, the energy levels of the nuclei Be^9 and Be^{10} can be identified directly. In addition, a measurement of the relative intensities of the reactions $Be^9(dd')Be^{9*}$ and $Be^9(d,p)Be^{10}$ for leaving the residual nucleus in any given state can be obtained.

C. Beam Energy Measurement and Energy Calibration

A 2-mil polyethylene target was used for determining the incident deuteron beam energy. When the deuterons impinge upon the target among the reaction particles emitted are the protons from the reactions $C^{12}(d,p)C^{13}$ ($Q=2.723$) and $C^{12}(d,p)C^{13*}$ ($Q=-0.370$).[5] With an aluminum absorber in front of the counter and counter at an angle of 45° with respect to the incident deuteron beam, the ratio of the proton energies was measured by a single-channel pulse-height analyzer. Since this ratio is a sensitive function of deuteron beam energy, it was possible to measure the latter fairly accurately.

After the beam energy had been measured, the elastic deuterons coming from the C^{12} were observed at angles of 30° and 90°. Since these energies could be calculated, using the range-energy curves to correct for the counter thickness, it was possible to obtain a pulse height-scattered deuteron energy relationship. This was used to help identify the nuclear states involved in the (dd') reactions observed.

D. Angular Distribution Measurements

In order to avoid errors in obtaining the relative intensities of particle groups at different angles, the following procedure was used. With the target at an angle of 55° with respect to the beam, the deuteron pulse-height distribution was obtained by the particle selective counter at an angle of 40°. The shape and magnitude of the peak corresponding to the desired inelastic deuteron group was followed back to 90°, after which the peak was again run at 40°. Then the desired peak was followed as far forward as possible, and the 40° data were repeated a third time. To double

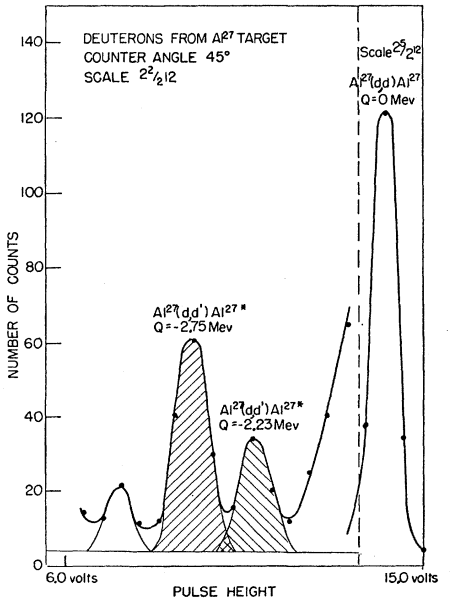

FIG. 7. Scattered deuteron energy spectrum from deuteron bombardment of Al^{27} target.

[5] F. Ajzenberg and T. Lauritsen, Revs. Modern Phys. 24, 321 (1952).

check, the peak was observed on both sides of the beam, the target being set normal to the beam for the purpose. By this means, the error in determining the angle which the counter makes with the beam was reduced to a minimum.

Before comparing the data with the theoretical angular distributions, the data were reduced to the center-of-mass system.

E. Cross-Section Measurements

Cross-section measurements were made by a comparison method, the differential cross section for the reactions $C^{12}(d,p)C^{13}$ ($Q=2.723$), $C^{12}(d,p)C^{13*}$ ($Q=-0.370$) and $C^{12}(d,p)C^{13*}$ ($Q=-1.18$) being used as a standard. The relationship employed was

$$\frac{d\sigma}{d\Omega}=\frac{C/N}{C_s/N_s}\frac{A/T}{A_s/T_s}\frac{\cos\phi}{\cos\phi_s}\frac{d\sigma}{d\Omega_s},$$

where $d\sigma/d\Omega$=differential cross section in mb/atom steradian, C=intensity of peak (area under differential spectrum curves), N=number of incident deuterons, measured by monitor counter, A=atomic weight of target, ϕ=angle target normal makes with deuteron beam, s=subscript denoting quantities relating to standard, and T=target thickness in mg/cm^2.

The cross sections were used mainly to get data of use in differentiating among the theories as to their relative feasibility. The accuracy of such measurements is discussed in Sec. F.

F. Experimental Uncertainties

The sources of error in the beam energy were small except for the variation of beam energy with the power level of the cyclotron. Since the deuteron beam intensity had to be reduced for forward angle measurements to avoid pulse pile-up, and increased for large-angle measurements to obtain the data in a reasonable time, this factor contributed perhaps ± 0.07 Mev. The total uncertainty ascribed to beam energy measurements was ± 0.1 Mev. It is expected that the (d,d') angular distributions do not greatly depend on energy when the deuterons are well above the nuclear barrier.

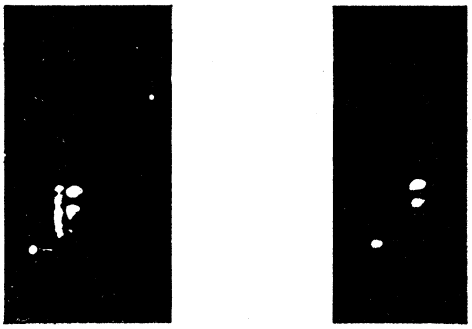

FIG. 8. Photographs of oscilloscope face showing separation of scattered protons and deuterons resulting from deuteron bombardment of Be^9. In the first photograph, protons are to the left; deuterons are to the right. In the second photograph, only deuterons are shown.

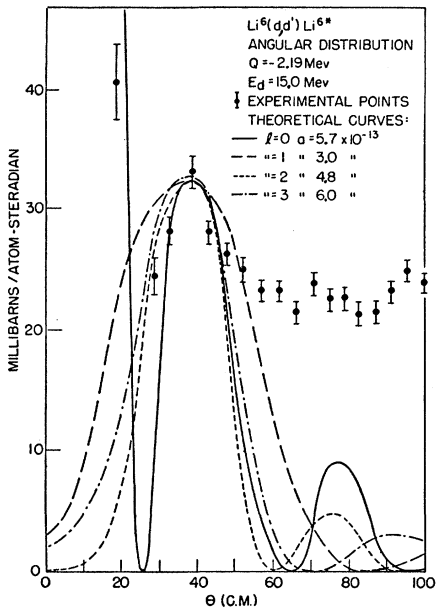

FIG. 9. Comparison of the angular distribution of inelastically scattered deuterons from the 2.19-Mev level of Li^6 with the curves predicted by the nuclear interaction theory.

The angular positions of the counter and the target were measured by balancing the output of two 10-turn, 30K (0.1% linearity) helipots against each other. The helipot setting corresponding to 0° was obtained by measuring the Rutherford scattering of deuterons from a thin gold target at different angles on both sides of the beam. The error in determining the zero angle, the finite area of the beam on the target, and the slight variation in beam direction with cyclotron power all contributed to the angular uncertainty of ± 1.0 degree.

The errors in particle selection were fortunately small. It was possible to set the mass pulse-height discriminator fairly accurately, since those protons which did "leak over" in the inelastic deuteron energy range had a continuous spectrum. The discriminator could be set accurately by observing this proton "background," and was checked before and after each angular distribution measurement.

The errors in determining the relative intensities of the inelastically scattered deuteron groups at different angles were perhaps the most important. The statistical error was the most important, especially at small angles. The monitor counter statistics and the variation of target thickness over its area added an estimated 10% error. The total uncertainties in determining the

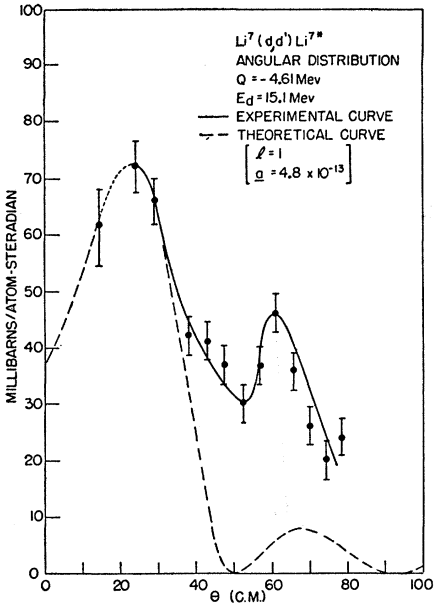

FIG. 10. Comparison of the $Li^7(d,d')Li^{7*}$ angular distribution with the nuclear interaction theory.

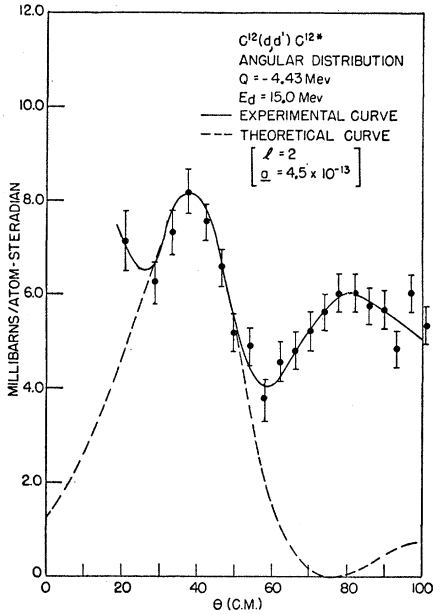

FIG. 12. Comparison of the $C^{12}(d,d')C^{12*}$ angular distribution with the nuclear interaction theory.

relative intensities at different angles are shown in the data, and include the above-mentioned factors.

The errors in cross-section measurements were unfortunately large. The largest contributor to this error was the energy thickness of the counter which made it impossible to observe the inelastic deuteron groups at angles much beyond 90°. The possible errors in beam energy determination and the accuracy of the standard cross sections added another 30%. The total cross-section measurements are not to be relied upon for accuracy greater than a factor of ± 2. Their purpose was to obtain information about the inelastic deuteron scattering process and not just to compile data.

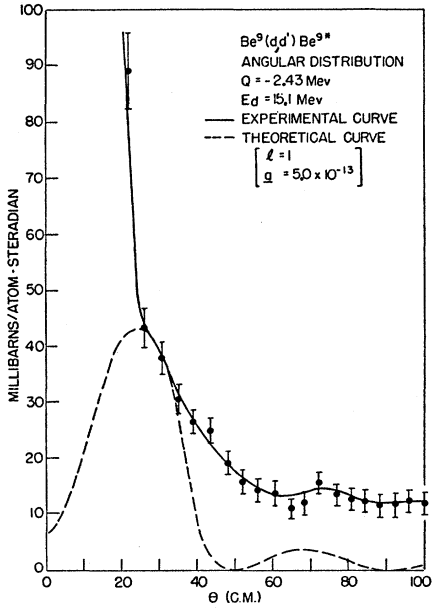

FIG. 11. Comparison of the $Be^9(d,d')Be^{9*}$ angular distribution with the nuclear interaction theory.

THEORIES ON INELASTIC DEUTERON INTERACTIONS

A. Nuclear Interaction Theory

This theory, published by Huby and Newns,[6] is somewhat analogous to the (d,p) theories of Butler[7] and others. It assumes that the probability of both constituents of the deuteron being simultaneously within the range of the nuclear forces can be neglected. The angular distribution to be expected in inelastic deuteron scattering reactions is derived from the Born approximation. The differential cross section is of the form

$$\frac{d\sigma}{d\Omega}(\phi)=\frac{2\pi}{\hbar}\left|\int \psi_f^* X_f^* X_{Df}^* V \psi_i X_i X_{Di} d\tau d\mathbf{R}_n d\mathbf{R}_p\right|^2,$$

where ψ_i = initial deuteron translational wave function, ψ_f = final deuteron translational wave function, X_i = initial nuclear wave function, X_f = final nuclear wave function, X_{Di} = initial internal deuteron wave function, X_{Df} = final internal deuteron wave function, and V = interaction potential between the neutron and the nucleus.

The integral can be evaluated, provided certain assumptions are made. These are: (1) The interaction potential operates only over a sphere of radius a. (2) The incident and scattered deuteron wave functions

[6] R. Huby and H. C. Newns, Phil. Mag. 42, 1442 (1951).
[7] S. T. Butler, Proc. Roy. Soc. (London) A208, 559 (1951).

are plane waves of wave numbers k_i and k_f, respectively. (3) The internal ground state of the deuteron is a pure triplet S state with a radial wave function of the form

$$(\epsilon-\alpha|\mathbf{R}_n-\mathbf{R}_p|)/|\mathbf{R}_n-\mathbf{R}_p|,$$

where $\alpha=(1/\hbar)\times(M_p\times\text{deuteron binding energy})^{\frac{1}{2}}=0.23\times10^{13}$ cm^{-1}.

Making these assumptions and substituting in the original equation, the following result is obtained:

$$\frac{d\sigma}{d\Omega}(\theta)=\sum\left\{|A_l{}^2|\left[\frac{4\alpha}{k}\tan^{-1}\left(\frac{k}{4\alpha}\right)\right]\left(\frac{\pi}{2ka}\right)^{\frac{1}{2}}J_{l+\frac{1}{2}}(ka)\right\}^2,$$

where $k=k_i-k_f$, $a=$radius beyond which the nuclear force field is considered to be zero, and $J(\ )=$regular Bessel functions of the first kind. The A^l's are unknown constants. The most important factor determining the angular distribution is

$$[J_{l+\frac{1}{2}}(ka)]^2/ka.$$

The rules which apply in applying the theory to specific cases are: (a) If l is even, there is no change of parity in the target nucleus; if l is odd, there is a parity change. (b) The final nuclear spin must satisfy the equation,

$$\mathbf{J}_f=\mathbf{J}_i+\mathbf{l}+\mathbf{1}.$$

It is noteworthy that this theory predicts relative minima in the forward direction except for the cases where $l=0$.

B. Electric Interaction Theory

This theory, published by Mullin and Guth,[8] assumes that the interaction between an inelastically scattered deuteron and the scattering nucleus is of an electrical nature. The interaction potential assumed is of the form

$$V=0, \qquad r\lesssim r_0,$$

$$V=\sum_{u=1}^{z}\frac{ze^2}{|\mathbf{r}-\mathbf{R}_\mu|}, \qquad r\gtrsim r_0.$$

where $r=$coordinate of the incident deuteron,

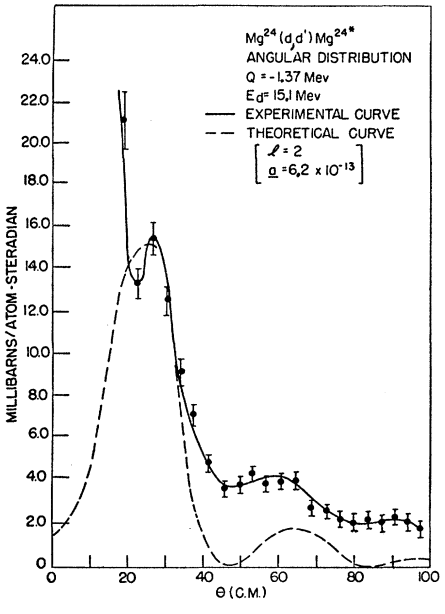

FIG. 13. Comparison of the $Mg^{24}(d,d')Mg^{24*}$ angular distribution with the nuclear interaction theory.

[8] C. J. Mullin and E. Guth, Phys. Rev. 82, 141 (1951).

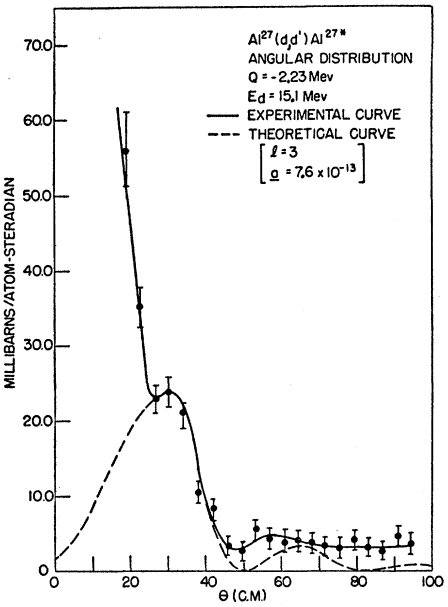

FIG. 14. Comparison of the $Al^{27}(d,d')Al^{27*}$ ($Q=-2.23$ Mev) angular distribution with the nuclear interaction theory.

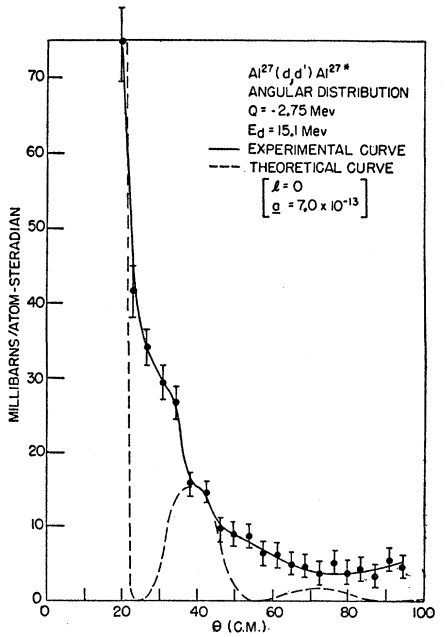

FIG. 15. Comparison of the $Al^{27}(d,d')Al^{27*}$ ($Q=-2.75$ Mev) angular distribution with the nuclear interaction theory.

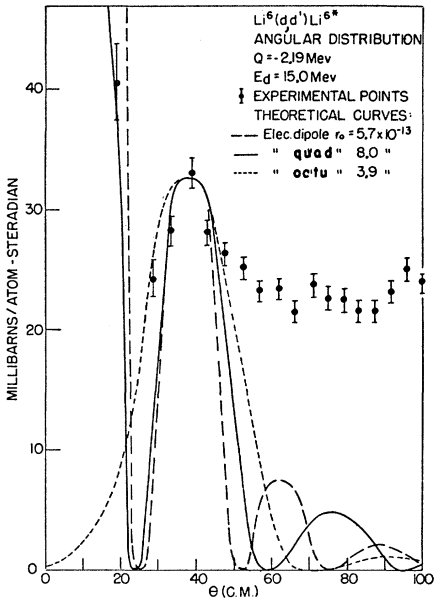

FIG. 16. Comparison of the angular distribution of inelastically scattered deuterons from the 2.19-Mev level of Li^6 with the curves predicted by the electric interaction theory.

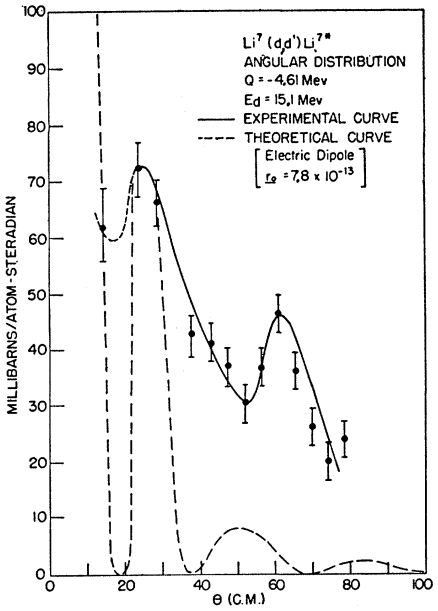

FIG. 17. Comparison of the $Li^7(d,d')Li^{7*}$ angular distribution with the electric interaction theory.

Z=atomic number of the scattering nucleus, r_0=radius at which the electric field of the nucleus is considered to arbitrarily go to zero, z=atomic number of the scattered deuteron, and R=coordinate of the μth particle in the nucleus. The derivation is somewhat involved, but the end result for the scattering cross section is

$$\frac{d\sigma}{d\Omega}=4\left(\frac{n_1}{Z}\right)^2\frac{k_1k_2}{2j_A+1}K^{2(l-2)}\left[\frac{j_{l-1}(Kr_0)^2}{(Kr_0)^{l-1}}\right]^2 M_{AB}{}^2,$$

where $n_1=zZe^2/\hbar v_1$, V_1=incident deuteron, k_1=incident wave number ($\mathbf{K}=\mathbf{k}_1-\mathbf{k}_2$), M_{AB}=multipole-matrix element for the nuclear transition $A\rightarrow B$, and $j(\ )$ =spherical Bessel functions. In the preceding, the deuteron translational wave functions were assumed to be plane waves.

The important factor determining the angular distribution is

$$K^{2(l-2)}\left[\frac{j_{l-1}(Kr_0)}{(Kr_0)^{l-1}}\right]^2.$$

TABLE I. Spins and parities of nuclear energy levels investigated.

Nucleus	Ground state	Excited state	l value possible
Li^6	1^+	$3^+(Q=-2.19)$	2
Li^7	3/2	$7/2(Q=-4.61)$	1,2,3
Be^9	$3/2^-$	$1/2(Q=-2.43)$	0,1,2
C^{12}	0^+	$2^+(Q=-4.43)$	2
Mg^{24}	0^+	$2^+(Q=-1.37)$	2
Al^{27}	5/2	$(Q=-2.23)$	?
Al^{27}	5/2	$(Q=-2.75)$	?

It is noteworthy that this theory predicts maxima in the forward direction for those cases where $l<3$.

C. Compound Nucleus Formation

It would be expected, because of the low binding energy of the deuteron, that the formation of a compound nucleus in (d,d') scattering would be extremely improbable. The success of the various theories of (d,p) interaction suggest that this is so. An article on the

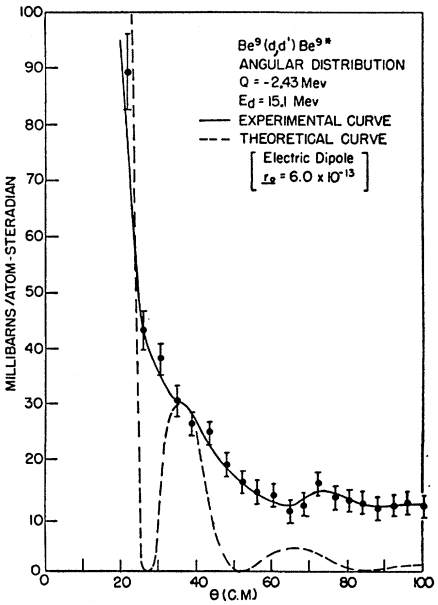

FIG. 18. Comparison of the $Be^9(d,d')Be^{9*}$ angular distribution with the electric interaction theory.

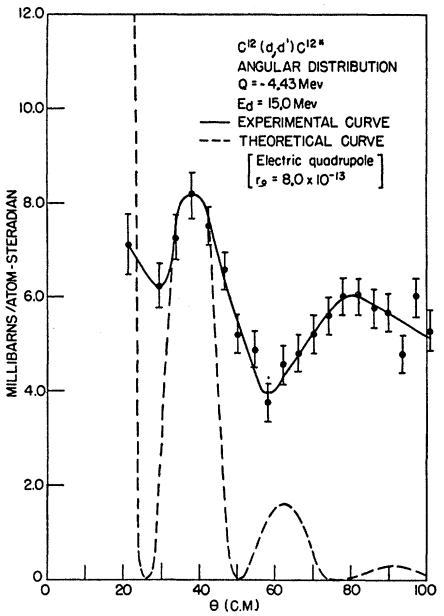

FIG. 19. Comparison of the $C^{12}(d,d')C^{12*}$ angular distribution with the electric interaction theory.

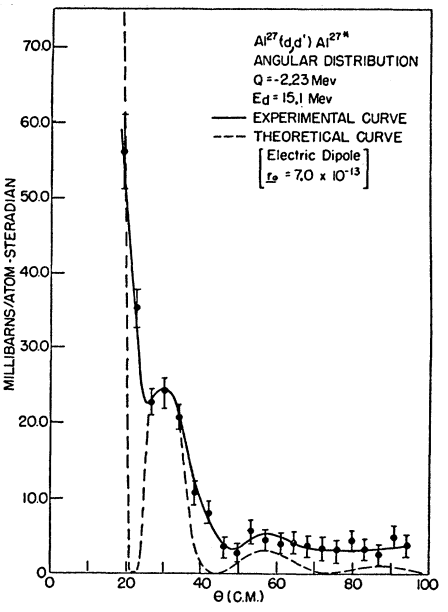

FIG. 21. Comparison of the $Al^{27}(d,d')Al^{27*}$ ($Q = -2.23$ Mev) angular distribution with the electric interaction theory.

cross sections to be expected for the formation of a compound nucleus by incident charged particles has been published.[9] However, the contribution due to individual nuclear levels cannot be obtained, only the total cross sections summed over all available nuclear levels being considered. In addition, postulates of the theory make its application somewhat questionable for light nuclei with few available levels. Evidence for the formation of a compound nucleus in dd' scattering would be: (1) approximately equal intensities at all angles; (2) a rear as well as a forward maximum, and (3) cross sections comparable to those of reactions known to proceed essentially by compound nucleus formations.

EXPERIMENTAL RESULTS

In Table I are listed the spins and parities[5] of the nuclear states involved in the observed reactions.

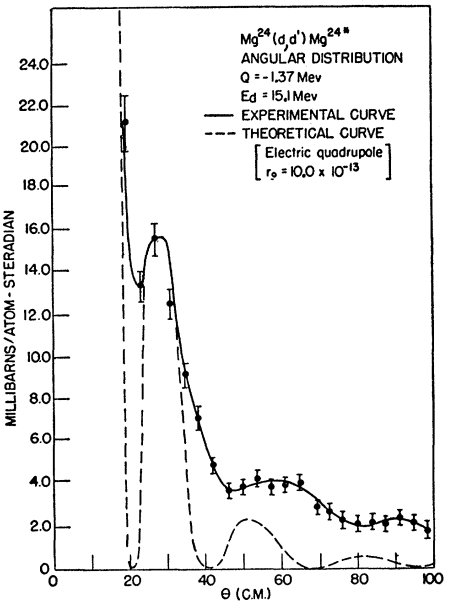

FIG. 20. Comparison of the $Mg^{24}(d,d')Mg^{24*}$ angular distribution with the electric interaction theory.

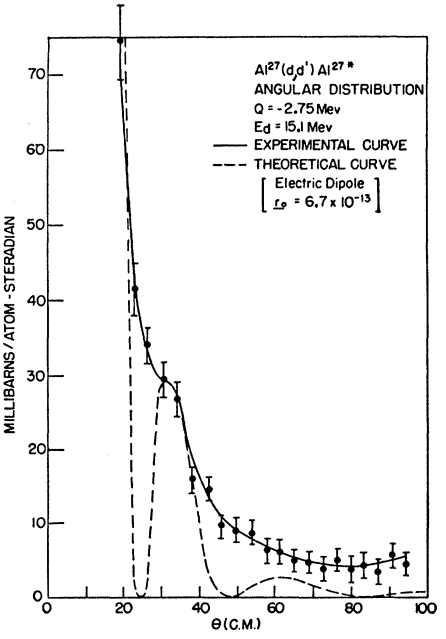

FIG. 22. Comparison of the $Al^{27}(d,d')Al^{27*}$ ($Q = -2.75$ Mev) angular distribution with the electric interaction theory.

[9] M. M. Shapiro, Phys. Rev. **90**, 171 (1953).

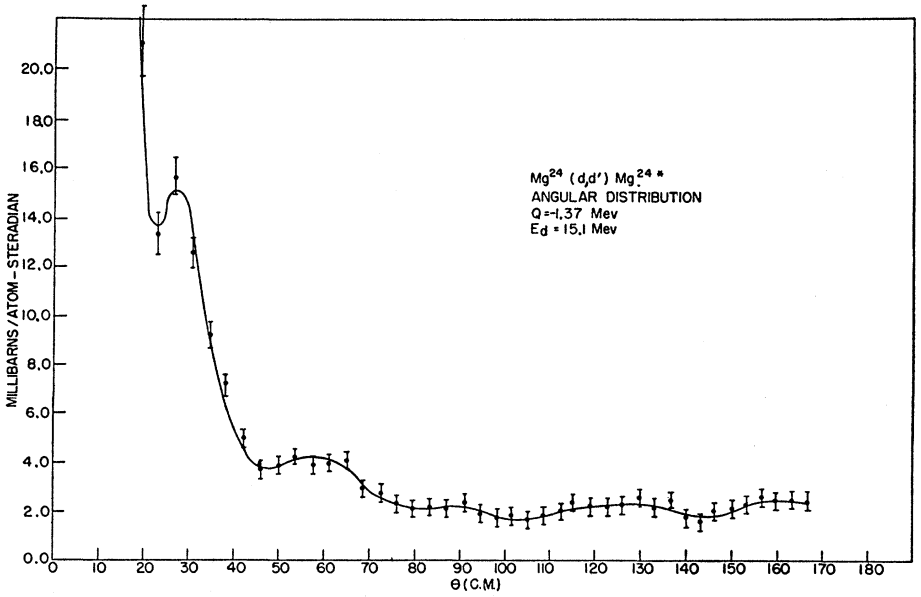

FIG. 23. Angular distribution of inelastic deuterons from the 1.37-Mev level of Mg^{24}, showing behavior at large angles ($\theta > 90°$).

A. Comparison with Nuclear Interaction Theory

The data corrected to the c.m. system are shown in Figs. 9 to 15 and compared with the curves predicted by the nuclear interaction theory. In Fig. 9, the theoretical curves for various l values are shown, together with the experimentally determined points. In Figs. 10 to 16, only the most reasonable theoretical curve is shown. With the exception of the $l=0$ curve, it is seen that the larger the l value the larger the value of a required to make the different curves fit.

The locations of the maxima and minima of the theoretical curves are seen to agree with the data better at large angles than at small.

B. Comparison with Electric Interaction Theory

The data are compared with the electric interaction theory in Figs. 17 to 23. The most important thing is the agreement between theory and experiment at small angles. It is to be noted, however, that the values of r_0, the radii of interaction required to fit the data, are much larger than the usual radii of the nuclei ($r=1.5\times10^{13}A^{\frac{1}{3}}$).

CONCLUSIONS

The theories are seen to be most applicable in the regions where the assumptions upon which they are based are most nearly valid. For small angles (large impact parameters), the electric interaction theory seems to fit the data better. The form of the potential assumed is valid only far enough from the nucleus so that the nuclear forces are not felt. For large angles, the nuclear interaction theory gives better agreement. The interaction potential assumed in this theory neglects interactions beyond a cut-off radius a. It may be possible to combine some of the features of both theories, using a potential which is electric from the nucleus and nuclear close in which will result in even better agreement with the data. Compound nucleus seems to be fairly unimportant for most (dd') reactions, apparently becoming only appreciable for very light nuclei.

The theories can be examined in more detail. The total measured cross sections (probably accurate to within a factor of 2) are compared in Table II with the values of M_{AB} (multipole moments) required to make the total cross sections agree. The expected and maximum theoretical total cross sections were computed

TABLE II. Nuclear multipole moments required, if electric interaction theory is to fully account for measured (d,d') cross sections.

Inelastic deuteron group (Q in Mev)	Total measured cross section (± a factor of 2)	Multipole moment M_{AB} required (± a factor of ~2)	Maximum multipole moment, theoretical[a]	Multipole moment M_{AB} expected theoretically[a]
$Li^6(Q=-2.19)$	310 mb	5.32×10^{-25}	2.24×10^{-25}	1.27×10^{-26}
$Li^7(Q=-4.61)$	718 mb	1.05×10^{-11}	8.61×10^{-13}	6.02×10^{-14}
$Be^9(Q=-2.43)$	212 mb	4.86×10^{-12}	1.25×10^{-12}	6.65×10^{-14}
$C^{12}(Q=-4.43)$	96 mb	1.84×10^{-25}	7.09×10^{-25}	2.00×10^{-26}
$Mg^{24}(Q=-1.37)$	88 mb	2.20×10^{-25}	2.24×10^{-24}	3.18×10^{-26}
$Al^{27}(Q=-2.23)$	107 mb	5.10×10^{-12}	5.85×10^{-12}	9.45×10^{-14}
$Al^{27}(Q=-2.75)$	145 mb	2.78×10^{-12}	5.85×10^{-12}	9.45×10^{-14}

[a] J. M. Blatt and V. F. Weisskopf, *Theoretical Nuclear Physics* (John Wiley and Sons, Inc., New York, 1952).

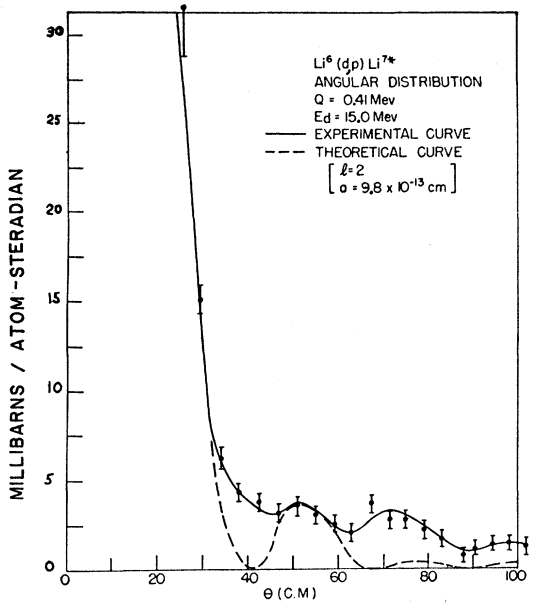

FIG. 24. Comparison of the $Li^6(d,p)Li^{7*}$ angular distribution with the nuclear interaction theory.

from the formula

$$M=3eR^l/(4\pi)^{\frac{1}{2}}(l+3) \quad \text{expected},$$
$$M_{lm}=ZeR^l \quad \text{maximum}.$$

The fact that the multipole moments required to make the electric interaction theory account for the phenomenon of inelastic deuteron scattering are larger than the maximum expected theoretically indicates that electric interaction is not the only process operating, at least for the Li^6, Li^7, and Be^9 nuclei.

There are two facts which indicate that the process by which deuterons are scattered inelastically is not the same as the process responsible for (d,p) and (d,n) reactions. The first fact comes from the comparison of the (d,p) and the (d,d') cross sections. The ratio of protons to the inelastic deuterons observed from the deuteron bombardment of Mg^{24} at 45° was measured to be 21. If (d,n) processes are comparable to (d,p) processes, the ratio becomes

$$(\Sigma\sigma_{dp}+\Sigma\sigma_{dn})/\Sigma\sigma_{dd'}=42.$$

The second fact is shown in the comparison of (d,d') with (d,p) and (d,t) angular distributions obtained with the same apparatus. The Born approximation has been used to obtain angular distributions for these interaction processes by a method similar to the nuclear interaction theory for (d,d') scattering.[10] The theory obtained has been compared with the data obtained for the following reactions at 15 Mev:

$Li^6(d,p)Li^{7*}$ $Q=0.41$ (Li^{7*} left in 4.67-Mev level),

$Li^7(d,t)Li^6$ $Q=-0.99$ (residual nucleus left in the ground state)

$Be^9(d,t)Be^8$ $Q=4.59$

[10] H. C. Newns, Proc. Phys. Soc. (London) **A65**, 916 (1952).

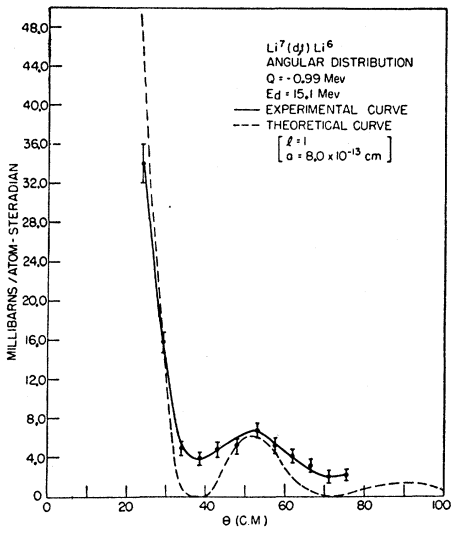

FIG. 25. Comparison of the $Li^7(d,t)Li^6$ angular distribution with the nuclear interaction theory.

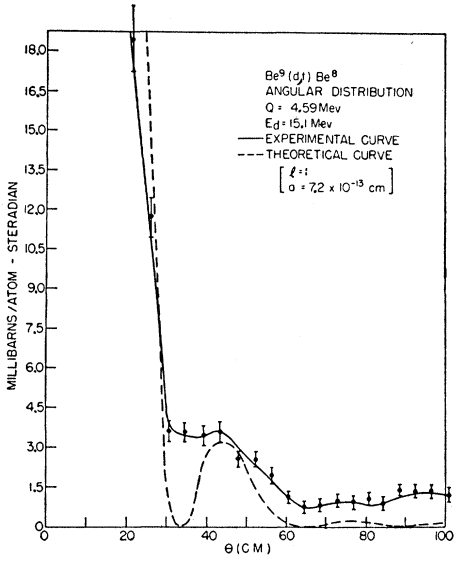

FIG. 26. Comparison of the $Be^9(d,t)Be^8$ angular distribution with the nuclear interaction theory.

It can be seen that the theories based upon the nuclear interaction process (see Figs. 24 to 26) fit the data better in each case than it did for the (d,d') reaction.

Further work with particles inelastically scattered from nuclei should make possible the more complete understanding of such interactions and their use as a tool for research.

ACKNOWLEDGMENTS

The author wishes to express his appreciation to Professor M. S. Livingston for his helpful suggestions concerning this work. In addition, the assistance of F. A. Aschenbrenner, E. F. White, and the M.I.T. cyclotron group were quite valuable.